ChemPubSoc Europe

DOI: 10.1002/chem.201505121

CHEMISTRY A European Journal Full Paper

Antitumor Agents

Asymmetric Synthesis and Binding Study of New Long-Chain HPA-12 Analogues as Potent Ligands of the Ceramide Transfer Protein CERT

Andrej Ďuriš,[a] Adam Daïch,*[b] Cécile Santos,[c] Laurence Fleury,[d] Frédéric Ausseil,[d] Frédéric Rodriguez,[c] Stéphanie Ballereau,[c] Yves Génisson,*[c] and Dušan Berkeš*[a]

Abstract: A series of 12 analogues of the Cer transfer protein (CERT) antagonist HPA-12 with long aliphatic chains were prepared as their (1*R*,3*S*)-*syn* and (1*R*,3*R*)-*anti* stereoisomers from pivotal chiral oxoamino acids. The enantioselective access to these intermediates as well as their ensuing transformation relied on a practical crystallization-induced asymmetric transformation (CIAT) process. Sonogashira coupling followed by triple bond reduction and thiophene ring hydrodesulfurization (HDS) into the corresponding alkane moieties was then implemented to complete the synthetic routes delivering the targeted HPA-12 analogues in concise 4- to 6-step reaction sequences. Ten compounds were evaluated regarding their ability to bind to the CERT START domain by using the recently developed time-resolved FRET-based homogeneous (HTR-FRET) binding assay. The introduction of a lipophilic appendage on the phenyl moiety led to an overall 10- to 1000-fold enhancement of the protein binding, with the highest effect being observed for a *n*-hexyl residue in the *meta* position. The importance of the phenyl ring for the activity was indicated by the reduced potency of the 3-deoxyphytoceramide aliphatic analogues. The 1,3-*syn* stereoisomers were systematically more potent than their 1,3-*anti* analogues. In silico studies were used to rationalized these trends, leading to a model of protein recognition coherent with the stronger binding of (1*R*,3*S*)-*syn* HPAs.

Introduction

Ceramides (Cer) are a wide family of key sphingolipids (SLs) formed by a sphingosine linked to a fatty acid through an amide bond. The sphingoid base can be of two main types (D-*erythro*-sphingosine or D-*ribo*-phytosphingosine), whereas other species such as dihydrosphingosine- and 6-hydroxy-sphinganine-based ceramides are also synthesized by human tissues.[1] On the other hand, the acyl moiety sometimes found to be unsaturated and/or hydroxylated is mostly a saturated C_{14}–C_{26} aliphatic chain (Figure 1). Cer are bioactive lipids that act as crucial mediators involved in the regulation of various cellular responses such as inflammation, cell migration, autophagy, differentiation, senescence, cell proliferation, and apoptosis.[2,3] Cer contribute to signal transduction cascades in affecting the lateral partition of membrane proteins through the dynamic assembly of lipid microdomains into signaling

[a] *Dr. A. Ďuriš, Dr. D. Berkeš*
Department of Organic Chemistry, Slovak University of Technology
Radlinského 981237, Bratislava (Slovak Republic)
Fax: (+33) 2-32-74-43-91
E-mail: dusan.berkes@stuba.sk

[b] *Prof. Dr. A. Daïch*
Normandie Univ, UNIHAVRE, CNRS, URCOM, 76600 Le Havre (France)
CNRS INC3M, FR 3038, EA 3221, UFR des Sciences et Techniques
25 rue Philippe Lebon, B.P. 1123, 76063 Le Havre Cedex (France)
Fax: (+33) 2-32-74-43-91
E-mail: adam.daich@univ-lehavre.fr

[c] *Dr. C. Santos, Dr. F. Rodriguez, Dr. S. Ballereau, Dr. Y. Génisson*
SPCMIB, UMR5068, CNRS-Université Paul Sabatier-Toulouse III
118 route de Narbonne, Toulouse, 31062 (France)
Fax: (+33) 5-61-55-60-11
E-mail: genisson@chimie.ups-tlse.fr

[d] *Dr. L. Fleury, Dr. F. Ausseil*
Unité de Service et de Recherche CNRS-Pierre Fabre n° 3388 ETaC
CRDPF, 3 avenue H. Curien, 31035, Toulouse cedex 01 (France)

Supporting information for this article is available on the WWW under http://dx.doi.org/10.1002/chem.201505121.

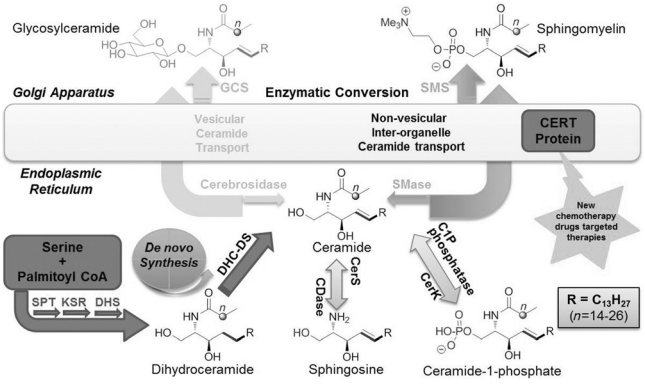

Figure 1. Sphingolipid metabolism and biosynthesis Scheme including the CERT protein.

platforms. They also act as second messengers in activating diverse intracellular kinases or phosphatases.

Cer are generated from palmitoyl-CoA and serine through a de novo biosynthetic pathway (Figure 1). Viewed as a metabolic hub, the resulting Cer are in equilibrium with ceramide-1-phosphate (C1P), glucosylceramide (GlcCer), sphingomyelin (SM), and sphingosine (Sph). Due to their rapid turnover, Cer homeostasis thus requires a fine balance between the synthesis and the degradation of these SLs. Alternatively, the Sph resulting from the hydrolysis of Cer can be phosphorylated into sphingosine-1-phosphate (S1P) that in turn may be irreversibly cleaved upon the action of a lyase.

To progress along the different synthetic or degradative pathways, the amphiphilic Cer have to be transported from one subcellular compartment to another. In particular, the de novo generated Cer in the endoplasmic reticulum (ER) are transferred to the Golgi apparatus to be transformed into SM (Figure 1) thanks to a Cer transfer protein (CERT), delivering its substrate to SM synthase in an energy-dependent manner.[4]

CERT protein is a cytoplasmic 68 kDa member of the START domain-containing protein family.[5] It is constituted of different domains and motifs, all important for its ER-to-Golgi ceramide trafficking function.[6] Among them, the steroidogenic acute regulatory protein (StAR)-related lipid transfer (START) domain holds a crucial role.[7] It is found at the carboxy-terminal region, and specifically recognizes and transfers the natural D-*erythro* isomer of Cer.

The CERT protein is emerging as a key player in several pathological processes. An increased CERT expression was observed in several drug-resistant cancer cell lines that could be re-sensitized to chemotherapeutic agents through genetic or pharmacological CERT inhibition.[8,9] CERT was shown to bind to serum amyloid P-component and to be present in brain amyloid plaques from Alzheimer disease patients.[10] Inhibition of CERT through its phosphorylation by protein kinase D negatively regulates hepatitis C virus secretion.[11,12] Finally, recruitment of CERT from host cells was demonstrated to be involved in the rerouting of SM toward parasitophorous vacuoles in the course of the development of obligate intracellular bacteria *Chlamydia Trachomatis*.[13,14] These different studies suggest that pharmacological inhibition of CERT could represent an innovative strategy in diverse therapeutic contexts.

HPAs (namely *N*-(3-hydroxy-1-hydroxy-methyl-3-phenyl-propyl)alkanamides as highlighted in Figure 2) represent the only class of CERT inhibitors reported to date. In 2001, Hanada and Kobayashi described HPA-12 (**1**, Figure 2), a derivative embedding a dodecanamide moiety, as a new inhibitor of intracellular Cer trafficking.[15,16] This precursory report was followed by the discovery by Hanada of the unique CERT protein-associated Cer transfer machinery.[17] HPA-12 was subsequently recognized as a protein antagonist. It specifically inhibits the CERT-mediated intracellular redistribution of fluorescent Cer analogues and the intermembrane Cer transport in a radioactivity-based cell-free assay system.[7]

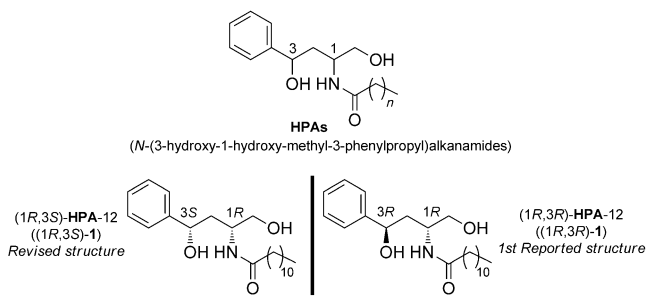

Figure 2. HPAs and HPA-12 structures.

HPA12 is now the benchmark CERT protein-targeting cellular inhibitor of de novo SM biosynthesis in various domains. It was used, for instance, to sensitize drug-resistant cancer cells lines overexpressing CERT to paclitaxel-induced apoptosis[8] or to attenuate the CERT-controlled hepatitis C virus activity through blockage of the virion production.[11]

Despite its widespread use, HPA-12 has led to only limited structure–activity relationship studies. Whereas the presence of both free hydroxyl groups proved necessary, the introduction of a secondary alcohol at the C-2 position of HPA-12 was not found to be beneficial for the cellular activity. Acyl chains comprised between C11 and C15 led to comparable inhibitory potency in a cell-based assay, whereas the presence of shorter or longer alkanamide fragments either diminished or suppressed the activity.[18] Early on, the configuration of the two stereocenters was shown to strongly affect the cellular inhibitory activity, the most potent of the four stereoisomers being initially recognized as the (1*R*,3*R*) isomer.[7] Crystal structures of a series of (1*R*,3*R*)-HPAs with C13 to C16 acyl chains in complex with the CERT protein START domain were reported, indicating a recognition mode very similar to that of Cer, the natural cargo lipid.[19] The configuration of the most active HPA-12 stereoisomer was, however, revised later on as (1*R*,3*S*),[20,21] thus leaving open the issue of its exact mode of binding to the CERT protein. Overall, the surprising scarcity of data on structure–activity relationships might be correlated, to some extent, to the lack of sufficiently flexible synthetic access to the HPA core structure.

No less than nine different synthetic routes to HPA-12 have been described to date, essentially focusing on the most active stereoisomer. Kobayashi's original synthetic work was based on an asymmetric Mannich-type reaction that led to important methodological achievements between 2001 and 2004.[15,18,22] In 2004, the preparation of the (1*R*,3*R*)-stereoisomer, based on the initial Kobayashi's assignment, was also reported from a β-sulfonamido unsaturated sulfoxide.[23] Seven years later, the revision of configuration from (1*R*,3*R*) to (1*R*,3*S*),[20] led to a regain of interest for HPA-12. (*S*)-Wynberg lactone, L-serine-derived Garner's aldehyde and aspartic acid were independently used as chiral pool-issued precursors.[23] Lately, diastereo- and enantiocontrolled syntheses of HPA-12 through the asymmetric Ru-catalyzed *N*-demethylative rearrangement of isoxazolidines were successively described.[25] The synthesis of the enantiomeric (1*S*,3*R*)- and diastereoisomeric (1*R*,3*R*)-HPA-12 were also reported.

In 2011, we described the first unified access to all stereoisomers of HPAs based on a crystallization-induced asymmetric

transformation (CIAT) technology using 1-phenylethylamine as a readily accessible chiral inductor.[20] This work led to the reassignment of the configuration of the most potent stereoisomer of HPA-12, subsequently confirmed by Kobayashi.[26,21] Recently, this practical stereodivergent route, which also proved useful for the synthesis of several new analogues, was applied to the first stereocontrolled preparation of the four stereoisomers of HPA-12 on a multigram scale.[27]

Optimization of HPA derivatives as CERT inhibitors and, a fortiori, identification of new antagonist chemotypes, have also been hampered by the lack of practical tools allowing the systematic binding evaluation of large series of ligands.[28] In line with our precursory study on the identification of the SM biosynthesis inhibitor jaspine B as a potential CERT antagonist,[29] we recently described the first time-resolved FRET-based homogeneous (HTR-FRET) binding assay for the CERT START domain that proved amenable to high throughput screening (HTS).[30] This in vitro protocol also allowed us to quantify the ligand–protein binding through the determination of EC_{50} values.

Given the emerging importance of the CERT-dependent SM biosynthesis inhibition in several pathological contexts, there is a growing interest for readily accessible CERT antagonists of optimized potency. It is indeed worthy of note that, almost 15 years after the initial report of HPA-12, no report has yet been made of a more efficient analogue. The synthetic, computational and biological tools we recently developed appeared ideally suited to address this issue. We present here a detailed report of the asymmetric preparation and the in-depth in vitro/in silico study of the binding of a series of HPA-12 analogues to the CERT START domain.

Results and Discussion

Chemistry

Several key structural features of the HPA backbone can be identified for pharmacological optimization. Among them, the potentially labile amide group may be the object of relevant alterations. We focused our study on the modification of the lipophilic portion of the HPA backbone. The influence of the phenyl ring decoration or its replacement has hardly been explored so far. Opportunities offered by such modifications are illustrated by the development of several families of related ceramide analogues embedding a benzene ring as a surrogate to the lipophilic chain of the sphingoïd backbone. Replacement of the *p*-nitro substituent present on the phenyl group of the acid ceramidase inhibitor B-13 (Scheme 1) by a primary amine resulted in a significant enhancement of Cer-mediated apoptosis induction.[31] In the P-drug series, a class of GCS inhibitors, the introduction of an ethylenedioxy unit onto the phenyl ring led to a dramatic increase in inhibitory activity.[32] This modification resulted in the development of Eliglustat (Scheme 1),[33] which is commercialized by Genzyme for the treatment of Gaucher disease. In a preliminary set of experiments, we thus evaluated the CERT START domain recognition of several previously prepared (1*R*,3*S*)-*syn*-HPA-12 analogues using the FLINT binding assay we developed.[29] Replacement of the phenyl ring by a cyclohexyl residue did not noticeably alter the displacement of ceramide, whereas a *tert*-butyl moiety or cyclohexyl residue led to a strong diminution.[34] On the other hand, the introduction of a methoxy group in the *para* position significantly increased the level of protein binding.[34] These first observations thus prompted us to explore the impact of aromatic ring substitution further. In particular, we envisioned that this strategy could be advantageously exploited to introduce an aliphatic appendage (**14**, Scheme 1), likely to develop additional lipophilic interactions within the binding pocket. Inspection of the crystal co-structure of the CERT SART domain in complex with Cer or diacylglycerol derivatives indeed shows a conserved lipidic path along the cavity walls that could be exploited in this endeavor.[35]

To evaluate the impact of the rigid aromatic moiety within the skeleton, 3-deoxyphytoceramide analogues resulting from the formal deletion of the phenyl ring of HPAs were also envisioned (**15**, Scheme 1). Incorporation of rigid aromatic rings into the sphingosine aliphatic backbone of Cer and derivatives thereof was reported on several occasions. Bittman described

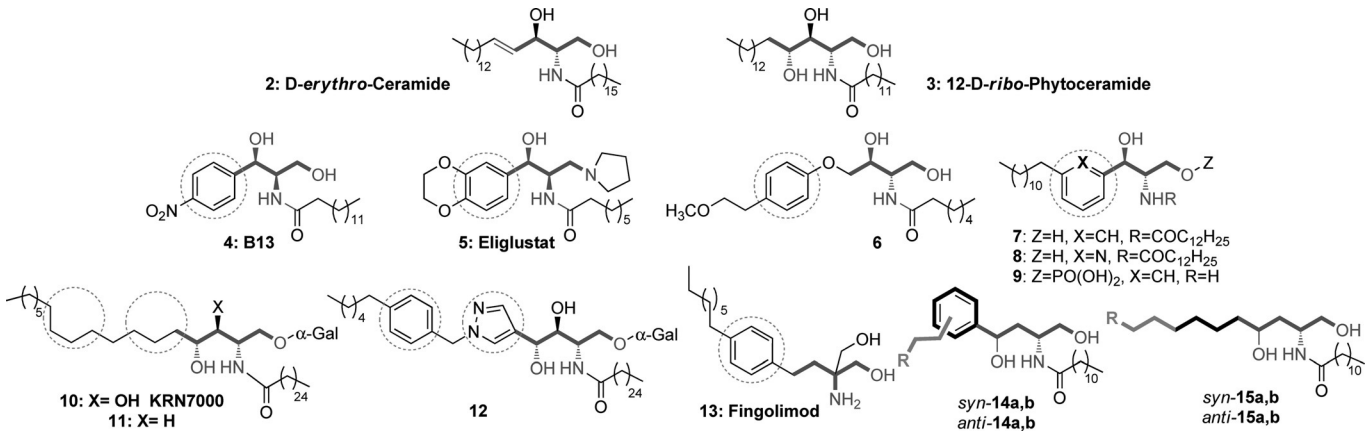

Scheme 1. Representative structures of conformationally constrained sphingosine and ceramide analogues and our target products **14a,b** and **15a,b** in both *anti* and *syn* forms.

a Cer analogue with the double bond of the sphingoïd base as part of the phenyl (or pyridyl) moiety (**7** and **8**, Scheme 1),[36] whereas Reissig reported the corresponding Cer-1-phosphate derivative (**9**, Scheme 1).[37] Delgado also published the solid phase synthesis of related phenyl ether-containing truncated Cer analogues (**6**, Scheme 1).[38] No biological activities were associated to these derivatives. On the other hand, Park described pharmacologically relevant modifications of the sphingosine backbone in a series of analogues of the immunostimulatory α-galactosylphytoceramide KRN7000 (**10**–**12**, Scheme 1).[39] The combined presence of a pyrazolo moiety and a phenyl ring in a specific position of the lipophilic chain of the Cer backbone of **12** led to a significantly enhanced activity in an autoimmune animal model. The development of FTY720, which culminated in the commercialization by Novartis of the immunosuppressant drug Fingolimod (**13**, Scheme 1), also fully illustrates the critical gain of a phenyl ring judiciously located along the aliphatic chain of the sphingosine backbone of sphingolipid-inspired lead structures.[40]

The overall strategy employed here to access the HPA-12 analogues **14a**,**b** and **15a**,**b** is depicted in Scheme 2. One of the central features of our approach is the use of alkyne and/or thiophene moieties to facilitate the branching of the lipophilic

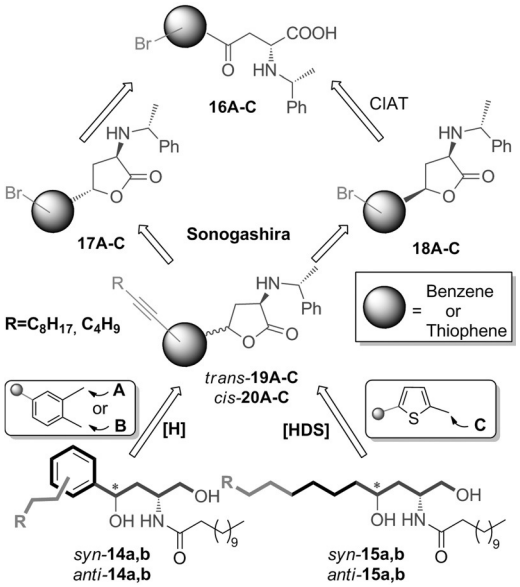

Scheme 2. Stereodivergent approach to the starting *trans*- and *cis*-bromo-substituted 2-aminobutanolides **17A**–**C** and **18A**–**C** as the key intermediates of the synthesis of the target products **14a**,**b** and **15a**,**b**.

appendage and in turn serve as an aliphatic fragment surrogate. The stereocontrolled entry to the HPA scaffold relied on a practical crystallization-induced asymmetric transformation (CIAT) leading to bromoarene-containing 2-aminobutanolides. Sonogashira coupling followed by triple bond reduction and thiophene ring hydrodesulfurization (HDS) into the corresponding alkane moieties was then implemented to complete the synthetic routes delivering the targeted HPA-12 analogues in concise 4- to 6-step reaction sequences.

Key to the preparation of these HPA-12 analogues was thus the straightforward access to the stereoisomerically pure *m*- or *p*-bromophenyl- and 5-bromothiophene-2-yl-substituted oxoamino-acids **16A**–**C**, secured from readily available starting materials through an efficient CIAT process[41] (Scheme 2). The stereodivergent conversion of the oxoamino-acids **16A**–**C** into the *trans*- or *cis*-2-amino-butanolides **17A**–**C** and **18A**–**C**, respectively, was in turn realized on gram-scale.

Worthy of note, the *syn*-hydroxyaminoacids required for the *N*,*N*-dicyclohexylcarbodiimide (DCC)-mediated cyclization into the (1*R*,3*S*)-*trans* lactones **17A**–**C**[42] were obtained through the highly stereoselective (diastereomeric ratio (d.r.) > 97:3) $MnCl_2$-catalyzed ketone reduction of the appropriate oxoamino-acids **16A**–**C** with sodium borohydride (Scheme 3).[43] In contrast, the

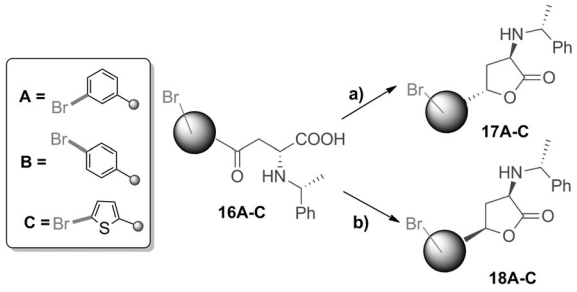

Scheme 3. Sequence for the synthesis of **17A**–**C** and **18A**–**C**. Reagents and conditions: a) 1) $NaBH_4$/cat. $MnCl_2 \cdot 4H_2O$, MeOH 0–5 °C, d.r. 97:3; 2) DCC, TEA, THF, RT, d.r. 97:3, overall yield for **17A** 67%, for **17B** 48%, and for **17C** 63%; b) 1) $NaBH_4$, MeOH RT, d.r. 2:1; 2) 8 M HCl, 60 °C, CIAT, d.r. 98:2, overall yield for **18A** 70%, for **18B** 66% and for **18C** 71%.

(1*R*,3*R*)-*cis* diastereoisomers **18A**–**C** were selectively prepared in a two-step one-pot procedure starting with the non-stereoselective sodium borohydride reduction of oxoamino-acids **16A**–**C** (d.r. = 2:1) followed by an acid-catalyzed lactonization (8 M HCl, 40 °C, 24 h; Scheme 3) under epimerizing conditions.[41d] The brominated aminobutanolides **17A**–**C** and **18A**–**C** were finally isolated by flash chromatography in high diastereomeric purity (d.r. > 99:1 in all cases).

A Pd^0-catalyzed Sonogashira cross-coupling[44] reaction followed by the saturation of the alkynyl moiety was envisioned as a flexible strategy for the introduction of the aliphatic appendage of the targeted HPA-12 derivatives. The literature predominantly reports the use of an alkynyl unit as a precursor of the olefin moiety of various linear[45] and constrained[46] ceramide analogues as well as α-galactosyl[47] derivatives. The partial reduction of an alkynyl fragment into an *E*-alkenyl unit was also used in the synthesis of the GlcCer synthase inhibitor PDMP[48] and analogues thereof, as well as that of sphingadienines and diverse aromatic ceramide analogues.[49] The introduction of an alkynyl unit as an alkyl fragment surrogate was, however, only scarcely exploited in the field of lipid synthesis. It was for instance used in the preparation of the anhydrophytosphingosine jaspine B (pachastrissamine) and analogues thereof, a series of cytotoxic inhibitors of the SM biosynthesis.[50]

After an extensive screening of experimental conditions by varying the catalyst ([$PdCl_2(Ph_3P)_4$], [$Pd(Ph_3P)_4$]), the solvent (THF, DMF, triethylamine (TEA)), the ratio of the reagents and the reaction temperature (Table 1), the best reaction conditions for the Sonogashira coupling[44] were the use of 3 equivalents of alkyne, 5 mol% of tetrakis-(triphenyl-phosphine)palladium ([$Pd(Ph_3P)_4$] along with 10 mol% of CuI as catalysts and Et_3N (12 mL per 1 mmol of lactone reactant) heated at reflux. The tertiary amine was opportunely employed as both the base and the solvent. Under these optimized conditions, the reaction proved effective for either aromatic or aliphatic alkyne partners and, except in the ^{t}Bu-substituted series **C**, all Sonogashira coupling products *trans*-**19A–C** and *cis*-**20A–C** were isolated in fair to good yields (Table 1). In the case of 3,3-dimethylbut-1-yne (R = ^{t}Bu, entry 3, Table 1), because of the low boiling point of the alkyne (b.p. 37–38 °C), the yields ranged from 30% up to 55%, independently of the halide used (series A or B) and despite variations of the experimental conditions, including notably an increase of the reaction temperature.

Having in hand the required enantiopure lactones *trans*-**19A–C** and *cis*-**20A–C** embedding the alkynyl and thiophenyl moieties as masked aliphatic fragments, we were in a position to complete the preparation of the targeted HPA-12 analogues **14a,b(A–C)**, **15a,b(A–C)** through the implementation of straightforward 3-step reaction sequences starting with the lactone reductive opening.[20]

We first addressed the benzenic series **A** and **B** (Scheme 4). The reduction of lactones *trans*-**19A,B** and *cis*-**20A,B** under optimized reaction conditions (10 equiv $NaBH_4$, EtOH, RT, 2–7 h) delivered the expected amino diols **19A–C** and **20A–C** with high yields of the isolated product (58–80%) (Scheme 4). Interestingly, no trace of the intermediate lactol was ever detected

Table 1. Sonogashira coupling reaction applied to the synthesis of 5-(alkynylaryl)-2-amino butanolides *trans*-**19A–C** and their diastereoisomers *cis*-**20A–C**.[a]

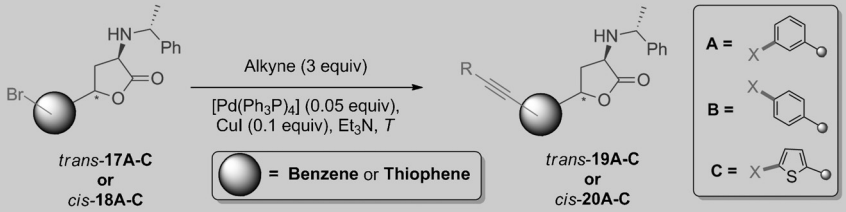

Entry	Product	R group	T [°C][b]	Yield of *trans*-**19A–C** [%]			Yield of *cis*-**20A–C** [%]		
				19A	**19B**	**19C**	**20A**	**20B**	**20C**
1	**a**	C_8H_{17}	90	83	72	72	85	86	77
2	**b**	C_4H_9	50	69	42	83	67	70	62
3	**c**	^{t}Bu	RT	60	51	69	30	31	55
4	**d**	Ph	90	82	71	75	85	70	68
5	**e**	PMP	70	72	86	68	79	83	56

[a] The reaction was monitored by TLC using a mixture of hexane and EtOAc as the eluent. [b] Yields of the isolated product after flash chromatography purification on silica gel column using the mixture of hexane and EtOAc as the eluent.

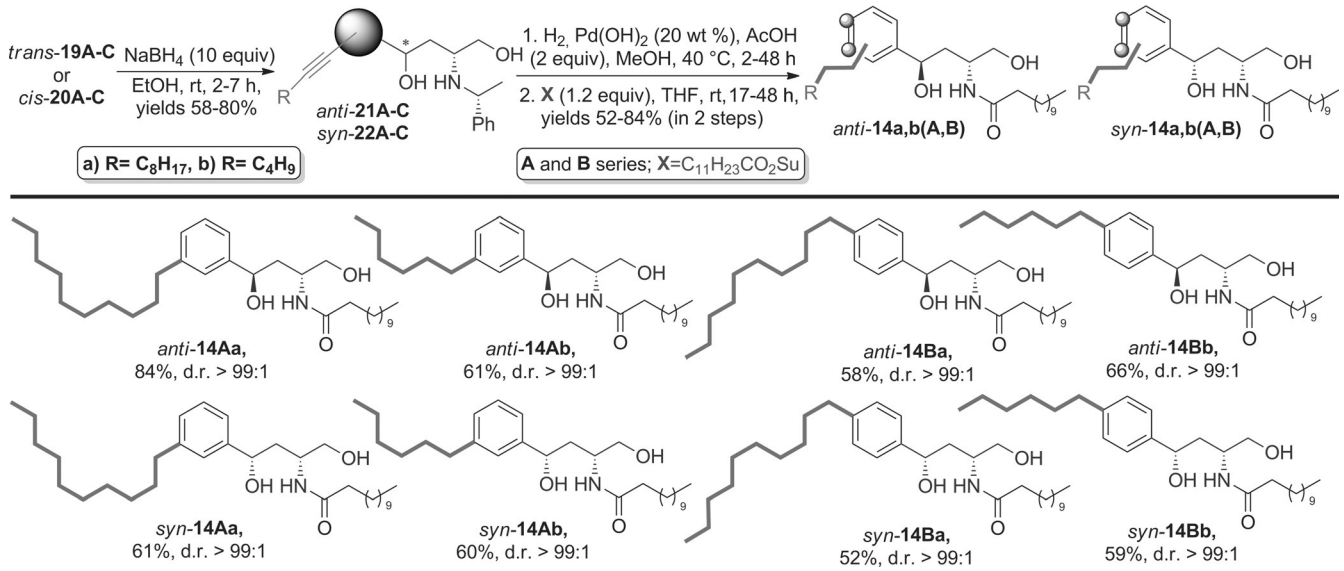

Scheme 4. Sequence for the synthesis of HPA-12 analogues *anti*-**14a,b(A,B)** and *syn*-**14a,b(A,B)** containing substituted alkyl chain on the benzene ring.

in the final reaction mixture. Furthermore, the transformation proceeded without erosion of the stereoisomeric purity of the starting *trans*- or *cis*-lactones. The relative configuration of the obtained *N*-alkyl aminobutanediols was determined from the ^{1}H NMR analysis of *trans*-**21 A**,**B** and *cis*-**22 A**,**B** (coupling constant analysis) based on our earlier findings regarding HPA-12 diastereomers[20] as well as other later studies using the same protocol.[24a,51]

The hydrogenolysis of *N*-benzylamines *trans*-**21 A**,**B** and *cis*-**22 A**,**B** then proceeded smoothly with concomitant hydrogenation of the triple bond under catalytic reaction conditions (1 atm, H_2 (balloon), 20 mol% $[Pd(OH)_2]$/C, 2 equiv AcOH, 40 °C, MeOH) to provide the corresponding saturated aminodiols. Interestingly this process is accelerated by the addition of two equivalents of glacial acetic acid, which also improved the diastereoisomeric purity of the isolated products (d.r. > 95:5) (Scheme 4).

The final N-acylation step was then carried out in a one-pot sequence without isolation of the primary amines. The use of *anti*-**21 a**,**b(A**,**B)** and *syn*-**21 a**,**b(A**,**B)**, respectively, with succinimide dodecanoate **X** (1.2 equiv) under neutral conditions (THF) smoothly provided the expected dodecanamides *anti*-**14 a**,**b(A**,**B)** and their diastereoisomers *syn*-**14 a**,**b(A**,**B)**. The targeted HPA-12 analogues were isolated after purification by chromatography in 52–84% yields over two steps and with d.r. > 99:1 (Scheme 4).

We then addressed the series **C** embedding a thiophene moiety (Scheme 5). As mentioned earlier, this heterocycle may be advantageously introduced as a masked *n*-butyl fragment thanks to the well-established reductive desulfurization protocol. The potential of this approach is illustrated in the literature[52] with examples in different fields of organic chemistry including stereoselective total synthesis.[53] Our plan was to convert directly the ethynylthiophene fragment into a linear 6-carbone aliphatic unit in a single operation. Interestingly, to our knowledge, no precedent for such a reductive process, combining the hydrogenation of an alkyne unit and the HDS of a thiophene ring, has so far been described in literature. Only rare reports of the reduction of a substituted vinylthiophene into the corresponding *n*-hexyl fragment were found.[54]

The substituted ethynylthiophene *anti*-**21 Ca**, selected as a model substrate, was subjected to Raney-Ni, a common reagent for reductive desulfurization.[55] Ethynylthiophene (1 mmol) was treated with activated Raney-Ni (5 wt equiv) in anhydrous methanol (4 mL) under 1 atmosphere of hydrogen. After stirring at room temperature for 24 h, purification by flash chromatography delivered the reaction product with 72% yield. Gratifyingly, the latter was identified as the aliphatic aminodiol *anti*-**23 a** resulting from the concomitant reduction of the carbon–carbon triple bond and the reductive desulfurization of the thiophene ring. The same protocol was successfully applied to substituted ethynylthiophene derivatives *anti*-**21 Cb**, *syn*-**22 Ca**, and *syn*-**22 Cb**. The expected aliphatic aminodiols *anti*-**23 b**, *syn*-**24 a**, and *syn*-**24 b** were isolated with 73%, 51%, and 62% yields, respectively.

Finally, the aminodiols *anti*-**23 a**,**b** and *syn*-**24 a**,**b** were converted into the targeted 3-deoxyphytoceramides by using the one-pot N-debenzylation/N-acylation sequence developed earlier. The expected dodecanamides *anti*-**15 a**,**b** and *syn*-**15 a**,**b** isolated in 53–72% yields over two steps, were obtained with high stereochemical purity (Scheme 5).

With the aim of shortening the reaction sequence starting from the substituted ethynylthiophene *anti*-**21 Ca**,**b** and *syn*-**22 Ca**,**b**, we envisioned to combine the three consecutive reductive transformations in a single operation, that is, the saturation of the alkyne fragment, the hydrodesulfurization of the thiophene nucleus and the hydrogenolysis of the *N*-benzyl group. Compound *syn*-**22 Ca** was considered as a relevant substrate. It embeds indeed a masked C18 skeleton as the naturally occurring phytosphingosine. This ethynylthiophene derivative was treated under prolonged reductive desulfurization conditions before proceeding to the N-acylation reaction in the same reaction vessel. This one-pot sequence delivered the expected 3-deoxyphytoceramide *syn*-**15 a** in 36% yield (Scheme 6). Interestingly, the yield of this one-pot sequence compares favorably with that of the corresponding stepwise process (36% vs. 30.6% as in Scheme 5) for an otherwise comparable reaction time (60 h vs. 48 h).

The present synthetic approach thus provided a concise and modular access to enantiopure 3-deoxyphytoceramide deriva-

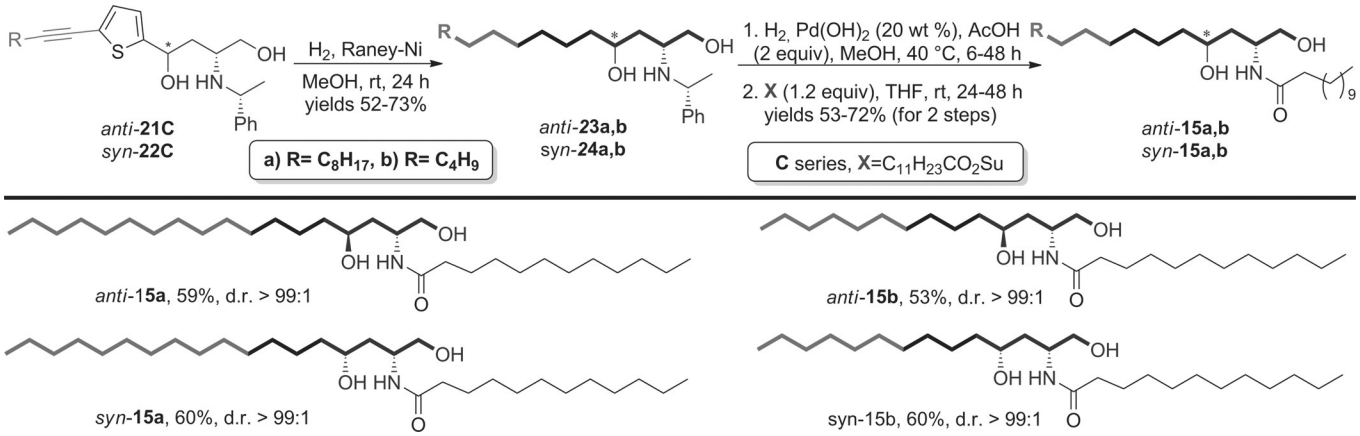

Scheme 5. Sequence for the synthesis of the target products *anti*-**15 a**,**b** and *syn*-**15 a**,**b** as 3-deoxyphytoceramide analogues.

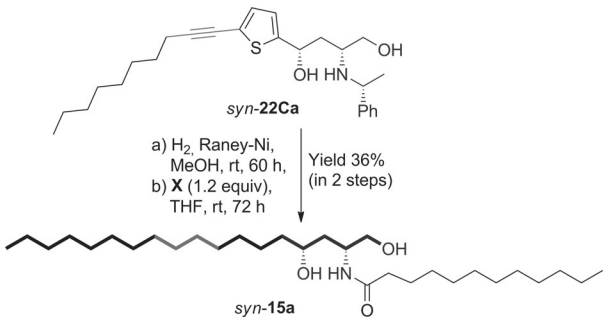

Scheme 6. One-pot synthesis of C_{18} 3-deoxyceramide *syn*-**15a** from alkyne *syn*-**22Ca** through the tandem reduction/debenzylation/acylation.

tives embedding different lipophilic tails. Interestingly, this particular sphingolipid backbone was advantageously exploited in the development of deoxygenated analogues of the α-galactosyl-ceramide KRN7000, a potent immunomodulator.[56] The importance of the 3-deoxyphytoceramide C18 skeleton as a relevant platform to develop new immunosuppressor agents thus further highlights the potential of our synthetic route.

Protein binding experiments

With the targeted HPA-12 derivatives in hand, we were in a position to evaluate their protein recognition capacities. We previously reported the first use of an HTR-FRET CERT START domain binding assay to quantify the relative protein interaction of the four HPA-12 stereoisomers.[27] The derivative of revised (1*R*,3*S*)-*syn* configuration proved to be the more affine, with an EC_{50} of 4 μM. In addition, both the 1*R* and 3*S* configurations were found to contribute equally to the extent of protein recognition, epimerization of either of these two stereocenters leading to a five- to six-fold increase in EC_{50} for both corresponding (1*S*,3*S*)- and (1*R*,3*R*)-*anti* derivatives.

Ten of the prepared HPA-12 analogues were subjected to the same binding assay. As can be seen from the EC_{50} values reported in Table 2, the introduction of a lipophilic fragment into the HPA-12 backbone gave rise to a 10- to 1000-fold enhancement in protein binding. The impact of the aliphatic substituent on the phenyl ring can be finely analyzed within the (1*R*,3*S*)-*syn* series. A *meta*-positioned lipophilic appendage led to a stronger recognition as compared to the *para*-substituted series (*syn*-**14Ab** vs. *syn*-**14Bb**, *syn*-**14Aa** vs. *syn*-**14Ba**). For a defined position, the protein recognition was also dependent on the alkyl chain length, with the lowest EC_{50} being observed, interestingly, for the hexyl-substituted analogues rather than for their decyl counterparts (*syn*-**14Aa** vs. *syn*-**14Ab**, *syn*-**14Ba** vs. *syn*-**14Bb**). Notably, the analogue *syn*-**14Aa** displayed an EC_{50} 1.49 nM, that is, three orders of magnitude lower than the HPA-12 itself. Overall, these trends were qualitatively conserved in the (1*R*,3*R*)-*anti* series with less pronounced gaps in protein binding between the different analogues.

Table 2. EC_{50} (nM) of CERT START domain protein binding for the prepared HPA analogues as determined by HTR-FRET assay.

Compound	EC_{50} [nM]
syn-HPA-12	4100
anti-HPA-12	22500
syn-**14Aa**	32.4
anti-**14Aa**	674
syn-**14Ab**	1.49
anti-**14Ab**	123
syn-**14Ba**	41.8
anti-**14Ba**	728
syn-**14Bb**	84.9
anti-**14Bb**	317
syn-**15b**	63.2
anti-**15b**	118

The **15** series of 3-deoxyphytoceramide derivatives, lacking the phenyl ring, also gave rise to potent protein binding. We previously identified C_{12}-D-*ribo*-phytoceramide as the best CERT START domain ligand in our FLINT experiments and an EC_{50} of 140 nM was found in our HTR-FRET assay (unpublished results). The activity of its 3-deoxy analogue, *syn*-**15a**, could not be evaluated because of its limited solubility. Truncated derivatives bearing a 14-carbon-long sphingosine backbone, however, gave rise to substantial protein binding with an EC_{50} of 63.2 nM for the (1*R*,3*R*) stereoisomer *syn*-**15b** (Table 2). The significantly lower binding of this derivative compared to that of its phenyl ring embedding analogue *syn*-**14Ab** clearly demonstrate the benefit of the aliphatic chain rigidification on protein recognition.

In concordance with our previous observations on the parent HPA-12 series, a strong influence of the configuration at C-3 on the protein binding was observed throughout this study. The 1,3-*syn* stereoisomers were systematically more active than their 1,3-*anti* congeners with a difference in EC_{50} of at least one order of magnitude. Interestingly, this gap in activity between the *syn* and the *anti*-stereoisomers is more pronounced that the five-fold ratio recorded with the original HPA-12 (EC_{50} 4 μM vs. 22 μM) and the largest difference in EC_{50} was recorded for the most active compound **14Ab** (1.49 nM vs. 123 nM) embedding a phenyl ring *meta*-substituted by an *n*-hexyl residue.

To further assess the biological potential of the most potent compound *syn*-**14Ab**, its effect on cell viability was evaluated in primary human fibroblast and compared to that of HPA-12 itself. In concordance with previous report,[16] the latter did not display any cytotoxicity at a concentration up to 10 μM. Most interestingly, under the same conditions, the 1000 times more active analogue *syn*-**14Ab** did not affect neither the cell viability of non-proliferative cells (see also the Supporting Information).

Molecular modeling analysis

Crystallographic structures of the CERT START domain co-crystallized with (1*R*,3*R*)-HPAs of various acyl chain length have been reported,[19] showing a strong similarity between the recognition mode of the inhibitor and that of the natural cargo lipid D-*erythro*-ceramide.[35] We previously developed a docking[57] method allowing the fine reproduction of the crystallographic co-structure of the protein and (1*R*,3*R*)-HPA-13 (Root-

Mean-Square Deviation (RMSD) of 0.79).[29] This in silico approach was also used to explore the possible modes of protein binding of the other HPA stereoisomers, including the most active (1*R*,3*S*) *syn*-derivative. This docking protocol was applied in the context of the present study in an attempt to rationalize the influence of the structural modifications of the HPA-12 analogues on their enhanced CERT SART domain protein binding.

We first focused on the less active *anti*-derivatives allowing a direct comparison with the experimental crystallographic data reported for the (1*R*,3*R*)-HPAs. Figure 3shows the reported X-ray co-structure between (1*R*,3*R*)-HPA-13 (in gray) and the CERT START domain in superimposition with the calculated complexes between the protein and the different *anti*-analogues evaluated (*anti*-**14 Aa**, *anti*-**14 Ab**, *anti*-**14 Ba**, *anti*-**14 Bb**, *anti*-**15 Ab**). In these minimized docked structures, the amide acyl chain follows a defined lipophilic path along the binding cavity wall distinct from the curved disposition seen in the X-ray co-structure. The orientation of the phenyl ring plane between HPA-13 and its *para*-substituted analogues shows a rotation of about 90° for the most active *meta*-substituted derivatives. Noteworthy, on the other hand, the polar head conformation of the ligand is highly conserved. Figure 4 A, showing the published X-ray co-structure of (1*R*,3*R*)-HPA-13 (in gray) and the CERT START domain in superimposition with a representative calculated complex of the *anti*-analogue of highest activity, *anti*-**14 Ab** (see the Supporting Information for a representation of the three complexes of lowest energy), clearly illustrates these trends. A closer analysis of the protein–ligand interactions (Figure 4 B) suggests that the polar head of *anti*-**14 Ab** develops a hydrogen bond network similar to that observed for the co-crystallized HPA-13 involving Glu446 (with the amide NH), Tyr553 (with the amide CO), Gln467 (with the primary OH) and Asn504 (with the secondary OH).

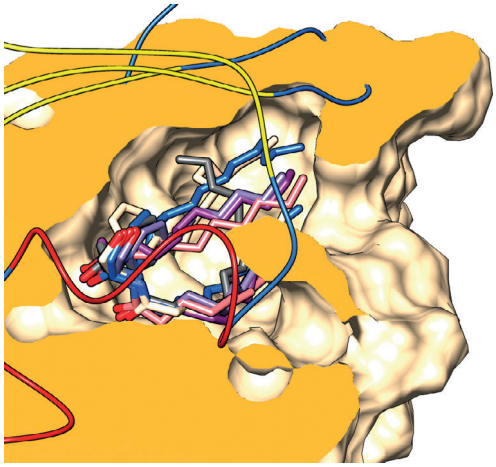

Figure 3. Superimposition of the docked poses of lowest energy of the anti-HPA analogues (**14Aa** (cream), **14Ab** (salmon), **14 Ba** (blue), **14 Bb** (purple), **15Ab** (pink)) with the reported (1*R*,3*R*)-HPA-13 crystallographic structure (gray). The orientation and protein surface (orange) clipping are chosen to show the placement of the polar heads of the lipids at the bottom of the binding site cavity.

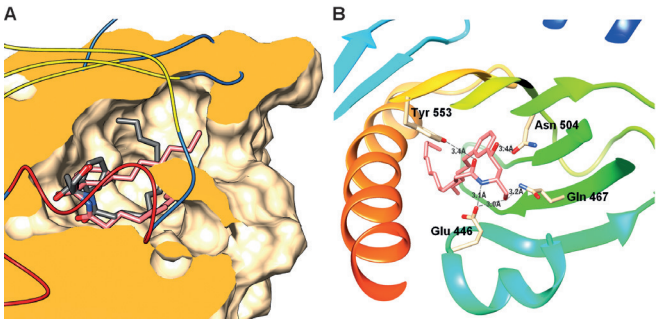

Figure 4. A) Superimposition of the docked pose of lowest energy of the HPA analogues *anti*-**14Ab** (pink) with the reported (1*R*,3*R*)-HPA-13 crystallographic structure (gray). B) Calculated hydrogen bond network in the docked pose with CERT START domain for *anti*-**14Ab**.

We then focused on the more active *syn*-configured series. Figure 5 Ashows a representative calculated complex of the most potent derivative *syn*-**14 Ab** (see the Supporting Information for a representation of the three complexes of lowest energy) superimposed with that of its analogue *anti*-**14 Ab** considered above (Figure 4).

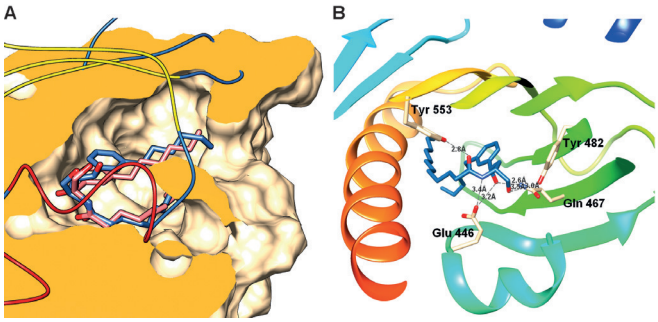

Figure 5. A) Superimposition of the docked poses of lowest energy of the HPA analogues *anti*-**14Ab** (salmon) and *syn*-**14Ab** (blue); B) Calculated hydrogen bond network in the docked pose with CERT START domain for *syn*-**14Ab**.

The *meta*-substituted phenyl ring plane is found to adopt the same twisted orientation (as compared to that of the original HPAs) in both *syn*- and *anti*-isomers, also driving the lipophilic chains along similar paths inside the binding cavity. In contrast, whereas the amide and primary alcohol fragments of the polar head present comparable spatial arrangements, the 3*S* secondary hydroxyl groups of *syn* isomer now points in a direction opposite to that of the 3*R* secondary alcohol of the diastereoisomer *anti*-**14 Ab**. This logically affects the hydrogen bond pattern developed by the polar head of the ligands in the more active *syn* series. As shown in Figure 5 B, whereas the amide portion still binds to Glu446 (by the amide NH) and Tyr 553 (by the amide CO), the interaction of the secondary OH with Asn504 is not available anymore. In place, a strong hydrogen bond network is apparent involving both hydroxyl groups, now pointing in the same direction as Glu446, Gln467, and Tyr 482 residues. Interestingly, this trend is observed throughout the entire *syn* series. The superimposition of the energetically

minimized complexes of the six analogues (*syn*-**14Aa**, *syn*-**14Ab**, *syn*-**14Ba**, *syn*-**14Bb**, *syn*-**15a**, and *syn*-**15b**) with the CERT START domain notably illustrates the conserved arrangement of the two hydroxyl groups (Figure 6). Also, the twist in phenyl ring plane orientation now affects both the *meta*- and *para*-substituted derivatives, being more pronounced for the analogues embedding a shorter aliphatic appendage.

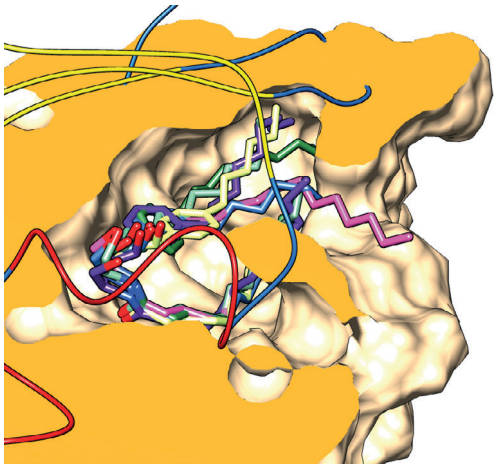

Figure 6. Superimposition of the docked poses of lowest energy of the *syn*-HPA analogues (*syn*-**14Aa** (purple), *syn*-**14Ab** (blue), *syn*-**14Ba** (dark green), *syn*-**14Bb** (pale yellow), *syn*-**15a** (pink), and *syn*-**15b** (pale green)).

Regarding the docking of the aliphatic series **15**, it is worthy of note that the C18 backbone of *syn*-**15a**, which could not be experimentally evaluated due to its reduced solubility, is found to be pointing in a direction similar to that of the sphingolipid skeleton of the natural D-*erythro*-ceramide in its X-ray crystallographic co-structure with the CERT START domain. As noted earlier, the aliphatic derivative *syn*-**15b** is a truncated 3-deoxy analogue of the C_{12}-D-*ribo*-phytoceramide tested in an earlier study. Both derivatives lead to a similar calculated complex of lowest energy, as can be seen in Figure 7. The phytoceramide, however, appears to develop a hydrogen bond between the C_2 hydroxyl group and Asn504 that is absent in its 3-deoxy analogues. The more than twofold stronger protein binding of *syn*-**15b** compared to that of the phytoceramide derivative (EC_{50} of 63.2 vs. 140 nM) thus suggests a limited contribution of this specific interaction to the overall protein binding of the ligand.

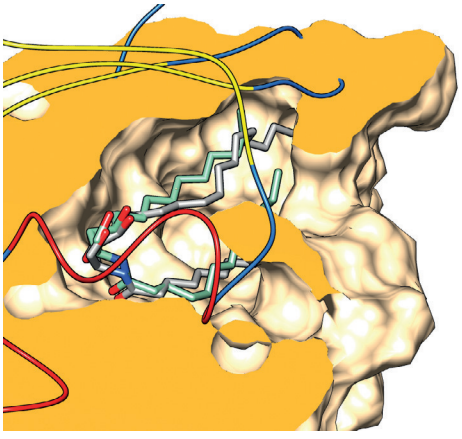

Figure 7. Superimposition of the docked poses of lowest energy of the HPA analogue *syn*-**15b** (pale green) and C12-D-*ribo*-phytoceramide (gray).

Altogether, the coherence of the protein interaction trends observed for each stereosiomeric series of these original HPA analogues allows to delineate unprecedented structure–activity relationships. A shorter aliphatic chain length and a *meta* branching position, both found to influence the protein binding favorably, also correlate with a more pronounced rotation in the ring plane orientation (as compared to the X-ray structure of (1*R*,3*R*)-*anti*-HPAs) in the calculated complexes of lowest energy. Most importantly, the significant gain in protein recognition associated with the 3*R* to 3*S* inversion of configuration of the HPA secondary alcohol would result from the establishment of a strongly stabilizing hydrogen bond network between both hydroxyl groups and Glu446, Gln467, and Tyr 482 residues. This would occur despite the loss of interaction with Asn504, known to be key to the binding of the D-*erythro*-ceramide natural ligand and also retained in the X-ray co-structure of (1*R*,3*R*)-*anti*-HPAs.

Conclusion

Access to a small library of HPA-12 analogues **14** and **15** was secured in four to six synthetic steps. The improved efficiency of our expedient crystallization-induced asymmetric transformation (CIAT) was both illustrated by the practical preparation of the enantio- and diastereoisomerically pure oxoamino-acid intermediates **16A–C** materials and by their subsequent transformation. The CIAT-based synthesis of *trans*- and *cis*-bromophenyl and 5-bromo-thiophene-2-yl substituted 2-amino-butanolides followed by Sonogashira coupling with appropriate aliphatic alkynes resulted in the formation of the array of arylethynyl 2-amino-butanolides *trans*-**19A–C** and *syn*-**20A–C** as key synthetic platforms.

In the benzenic series (**A** and **B**), the lactone reduction followed by the one-pot amine N-debenzylation/alkyne reduction/N-acylation sequence afforded the targeted *anti* and *syn* aliphatic chain-substituted HPA-12 analogues **14a,b(A,B)** in high stereoisomeric purity (d.r. > 99:1). The conciseness of this approach allowed a straightforward multigram access to these unique HPA-12 derivatives.

Application of this strategy to ethynylthiophene series (**C**) resulted, after concomitant alkyne hydrogenation/thiophene hydrodesulfurization and one-pot N-debenzylation/N-acylation, in a convenient enantioselective access to versatile 3-deoxyphytoceramide derivatives. Also, the 3-deoxyphyto-sphingosine core of these derivatives was found in the 3-deoxyanalogues of the potent immunomodulator α-galactosyl-phytoceramide (KRN7000). Along this line, a more concise and efficient approach to the 3-deoxyphytoceramide ***syn*-15a** bearing the naturally occurring 18-carbon chain was developed thanks to a one-pot procedure combining four different synthetic opera-

tions, that is, the alkyne reduction, the HDS process, the N-debenzylation, and the N-acylation.

Ten of the prepared HPA analogues were evaluated regarding their ability to bind to the CERT START domain using the recently developed HTR-FRET assay. The introduction of a lipophilic appendage on the phenyl moiety led to a 10- to 1000-fold enhancement of the protein binding compared to the corresponding unsubstituted HPA-12. The most favorable effect was recorded for the *n*-hexyl chain (vs. *n*-decyl) in the *meta* (vs. *para*) position. Data for the corresponding C14 aliphatic congeners also evidenced a beneficial influence on the protein recognition of the rigidification of the lipophilic appendage provided by the embedded aromatic ring. The 1,3-*syn* compounds were also systematically more potent than their corresponding 1,3-*anti* stereoisomers, in coherence with what was observed for the plain HPA-12. The gap in protein affinity was, however, more pronounced than in the original series, ranging from one to two orders of magnitude for the most active compounds. Docking experiments to the CERT START domain were carried out to gain insights into the rationalization of these structure–activity trends. According to calculated complexes of minimized energy, the long aliphatic tail of the sphingolipid-like backbone would orientate the overall arrangement of the lipophilic portions of the molecules. A favorable binding factor associated with the introduction of an aliphatic appendage might also lie in the induced twisted orientation of the phenyl ring plane as compared to what is found in the HPAs co-crystal structures. Most importantly, the epimerization of the 3*R* into the most active series of 3*S* stereoisomers would reshape the network of hydrogen bonds around the polar head of the ligand in a substantially distinct way from that of the natural cargo lipid D-*erythro*-ceramide. Altogether, it can be suggested that the additional aliphatic appendage, beyond the obvious gain in lipophilic interactions, would drive the ligands to adopt a restricted set of favorable bound conformations, reflected in both the overall affinity enhancement observed in the two diastereoisomeric series and the higher increase in binding efficiency of the *syn* stereoisomers over the corresponding *anti* derivatives. Importantly, this in silico study allowed for the first time to propose a model of protein recognition of the most active (1*R*,3*S*)-*syn* HPAs.

In delineating unprecedented structure–activity trends in the HPA series, this precursory study paves the way for the reasoned development of CERT antagonists with optimized inhibitory potency. Given the emerging importance of this ceramide transfer protein in various pathological contexts, the design of better inhibitors of the CERT-dependent SM biosynthesis is of great promise. Work along this line is currently underway in our laboratories, and the results will be published soon in a full account.

Acknowledgements

This work was supported by The Slovak Research & Development Operational Programfunded by the ERDF (ASFEU, ITMS 26220220093). The Scientific Council of the University of Le Havre (Normandie Université, France) and CNRS, INSERM, University of Paul Sabatier (France) and ANR (SphingoDR) are also gratefully acknowledged for their aids. We thank Pr. T. Levade from CRCT (Toulouse, France) for providing us the primary fibroblast cells.

Keywords: acylation · antitumor agents · enantioselectivity · sphingolipids · synthetic methods

[1] For dihydrosphingosine derivatives, see: G. Fabrias, J. Muñoz-Olaya, F. Cingolani, P. Signorelli, J. Casas, V. Gagliostro, R. Ghidoni, *Prog. Lipid Res.* **2012**, *51*, 82–94. For 6-hydroxysphinganine-based ceramide, see: A. Kováčik, J. Roh, K. Vávrová, *ChemBioChem* **2014**, *15*, 1555–1562.
[2] S. A. F. Morad, M. C. Cabot, *Nat. Rev. Cancer* **2012**, *13*, 51–65.
[3] Y. A. Hannun, L. M. Obeid, *Nat. Rev. Mol. Cell Biol.* **2008**, *9*, 139–150.
[4] T. Yamaji, K. Hanada, *Traffic* **2015**, *16*, 101–122.
[5] B. J. Clark, *J. Endocrinol.* **2012**, *212*, 257–275.
[6] K. Hanada, *Proc. Jpn. Acad. Ser. B* **2010**, *86*, 426–437.
[7] K. Kumagai, S. Yasuda, K. Okemoto, M. Nishijima, S. Kobayashi, K. Hanada, *Biochemistry* **2005**, *280*, 6488–6495.
[8] C. Swanton, M. Marani, O. Pardo, P. H. Warne, G. Kelly, E. Sahai, F. Elustondo, J. Chang, J. Temple, A. A. Ahmed, J. D. Brenton, J. Downward, B. Nicke, *Cancer cell* **2007**, *11*, 498–512.
[9] A. J. X. Lee, R. Roylance, J. Sander, P. Gorman, D. Endesfelder, M. Kschischo, N. P. Jones, P. East, B. Nicke, S. Spassieva, L. M. Obeid, N. J. Birkbak, Z. Szallasi, N. C. McKnight, A. J. Rowan, V. Speirs, A. M. Hanby, J. Downward, S. A. Tooze, C. Swanton, *J. Pathol.* **2012**, *226*, 482–494.
[10] C. Mencarelli, G. H. Bode, M. Losen, M. Kulharia, P. C. Molenaar, R. Veerhuis, H. W. M. Steinbusch, M. H. De Baets, G. A. F. Nicolaes, P. Martinez-Martinez, *J. Biol. Chem.* **2012**, *287*, 14897–14911.
[11] H. Aizaki, K. Morikawa, M. Fukasawa, H. Hara, Y. Inoue, H. Tani, K. Saito, M. Nishijima, K. Hanada, Y. Matsuura, M. A. C. Lai, T. Miyamura, T. Wakita, T. Suzuki, *J. Virol.* **2008**, *82*, 5715–5724.
[12] Y. Amako, G. H. Syed, A. Siddiqui, *J. Biol. Chem.* **2011**, *286*, 11265–11274.
[13] I. Derré, R. Swiss, H. Agaisse, *PLoS Pathog.* **2011**, *7*, e1002092–e1002092.
[14] C. A. Elwell, S. Jiang, J. H. Kim, A. Lee, T. Wittmann, K. Hanada, P. Melancon, J. N. Engel, *PLoS Pathog.* **2011**, *7*, e1002198–e1002198.
[15] M. Ueno, H. Kitagawa, H. Ishitani, S. Yasuda, K. Hanada, S. Kobayashi, *Tetrahedron Lett.* **2001**, *42*, 7863–7865.
[16] S. Yasuda, H. Kitagawa, M. Ueno, H. Ishitani, M. Fukasawa, M. Nishijima, S. Kobayashi, K. Hanada, *J. Biol. Chem.* **2001**, *276*, 43994–44002.
[17] K. Hanada, K. Kumagai, S. Yasuda, Y. Miura, M. Kawano, M. Fukasawa, M. Nishijima, *Nature* **2003**, *426*, 803–809.
[18] Y. Nakamura, R. Matsubara, H. Kitagawa, S. Kobayashi, K. Kumagai, S. Yasuda, K. Hanada, *J. Med. Chem.* **2003**, *46*, 3688–3695.
[19] N. Kudo, K. Kumagai, R. Matsubara, S. Kobayashi, K. Hanada, S. Wakatsuki, R. Kato, *J. Mol. Biol.* **2010**, *396*, 245–251.
[20] A. Ďuriš, T. S. Wiesenganger, D. Moravčíková, P. Baran, J. Kožíšek, A. Daïch, D. Berkeš, *Org. Lett.* **2011**, *13*, 1642–1645.
[21] S. Yasuda, H. Kitagawa, M. Ueno, H. Ishitani, M. Fukasawa, M. Nishijima, S. Kobayashi, K. Hanada, *J. Biol. Chem.* **2013**, *288*, 24162.
[22] a) S. Kobayashi, R. Matsubara, Y. Nakamura, H. Kitagawa, M. Sugiura, *J. Am. Chem. Soc.* **2003**, *125*, 2507–2515; b) S. Kobayashi, R. Matsubara, H. Kitagawa, *Org. Lett.* **2002**, *4*, 143–145.
[23] S. Raghavan, A. Rajender, *Tetrahedron* **2004**, *60*, 5059–5067.
[24] a) J. R. Snider, J. T. Entrekin, T. S. Snowden, D. Dolliver, *Synthesis* **2013**, *45*, 1899–1903; b) E. M. Saied, S. Diederich, C. Arenz, *Chem. Asian J.* **2014**, *9*, 2092–2094; c) J.-L. Abad, I. Armero, A. Delgado, *Tetrahedron Lett.* **2015**, *56*, 1706–1708; d) S. Chacko, M. Kalita, R. Ramapanicker, *Tetrahedron: Asymmetry* **2015**, *26*, 623–631.
[25] a) C. Z. Yao, Z. F. Xiao, X. S. Ning, J. Liu, X. W. Zhang, Y. B. Kang, *Org. Lett.* **2014**, *16*, 5824–5826; b) Z. F. Xiao, C. Z. Yao, Y. B. Kang, *Org. Lett.* **2014**, *16*, 6512–6514.
[26] M. Ueno, Y.-Y. Huang, A. Yamano, S. Kobayashi, *Org. Lett.* **2013**, *15*, 2869–2871.

[27] C. Santos, L. Fleury, F. Rodriguez, J. Markus, D. Berkeš, A. Daïch, F. Ausseil, C. Baudoin-Dehoux, S. Ballereau, Y. Génisson, *Bioorg. Med. Chem.* **2015**, *23*, 2004 – 2009.

[28] FRET or SPR-based in vitro assays were reported to quantify the intermembrane Cer transfer or the real-time Cer extraction activities, respectively, yet without application to the evaluation of inhibitors. For the FRET assay, see: J. Tuuf, M. A. Kjellberg, J. G. Molotkovsky, K. Hanada, P. Mattjus, *Biochim. Biophys. Acta Biomembr.* **2011**, *1808*, 229 – 235. For the SPR assay, see: T. Sugiki, H. Takahashi, M. Nagasu, K. Hanada, I. Shimada, *Anal. Biochem.* **2010**, *399*, 162 – 167.

[29] C. Santos, F. Rogriguez, V. Garcia, D. Moravcikova, D. Berkeš, A. Daïch, T. Levade, C. Baudoin-Dehoux, S. Ballereau, Y. Génisson, *ChemBioChem* **2014**, *15*, 2522 – 2528.

[30] L. Fleury, C. Faux, C. Santos, S. Ballereau, Y. Génisson, F. Ausseil, *J. Biomol. Screening* **2015**, *20*, 779 – 787.

[31] K. P. Bhabak, B. Kleuser, A. Huwiler, C. Arenz, *Bioorg. Med. Chem.* **2013**, *21*, 874 – 882.

[32] L. Lee, A. Abe, J. A. Shayman, *J. Biol. Chem.* **1999**, *274*, 14662 – 14669.

[33] J. A. Shayman, *Drugs Future* **2010**, *35*, 613 – 620.

[34] Unpublished results: See the Supporting Information.

[35] N. Kudo, K. Kumagai, N. Tomishige, T. Yamaji, S. Wakatsuki, M. Nishijima, K. Hanada, R. Kato, *Proc. Natl. Acad. Sci. USA* **2008**, *105*, 488 – 493.

[36] J. Chun, L. He, H.-S. Byun, R. Bittman, *J. Org. Chem.* **2000**, *65*, 7634 – 7640.

[37] V. Blot, U. Jacquemard, H.-U. Reissig, B. Kleuser, *Synthesis* **2009**, *5*, 759 – 766.

[38] S. Grijalvo, X. Matabosch, A. Llebaria, A. Delgado, *Eur. J. Org. Chem.* **2008**, 150 – 155.

[39] a) Y. Kim, J. Kim, K. Oh, D.-S. Lee, S. B. Park, *ACS Med. Chem. Lett.* **2012**, *3*, 151 – 154; b) Y. Kim, K. Oh, H. Song, D.-S. Lee, S. B. Park, *J. Med. Chem.* **2013**, *56*, 7100 – 7109.

[40] M. Kiuchi, K. Adachi, T. Kohara, M. Minoguchi, T. Hanano, Y. Aoki, T. Mishina, M. Arita, N. Nakao, M. Ohtsuki, Y. Hoshino, K. Teshima, K. Chiba, S. Sasaki, T. Fujita, *J. Med. Chem.* **2000**, *43*, 2946 – 2961.

[41] a) P. Jakubec, P. Petráš, A. Ďuriš, D. Berkeš, *Tetrahedron: Asymmetry* **2010**, *21*, 69 – 74; b) D. Berkeš, P. Jakubec, D. Winklerová, F. Považanec, A. Daïch, *Org. Biomol. Chem.* **2007**, *5*, 121 – 124; c) P. Jakubec, D. Berkeš, A. Kolarovič, F. Považanec, *Synthesis* **2006**, *23*, 4032 – 4040; d) D. Berkeš, A. Kolarovič, R. Manduch, P. Baran, F. Považanec, *Tetrahedron: Asymmetry* **2005**, *16*, 1927 – 1934.

[42] P. Jakubec, D. Berkeš, R. Šiška, M. Gardianová, F. Považanec, *Tetrahedron: Asymmetry* **2006**, *17*, 1629 – 1637.

[43] D. Berkeš, A. Kolarovič, F. Považanec, *Tetrahedron Lett.* **2000**, *41*, 5257 – 5260.

[44] For a general review on Songashira coupling reaction, see: a) R. Chinchilla, C. Nájera, *Chem. Rev.* **2007**, *107*, 874 – 922; b) R. Chinchilla, C. Nájera, *Chem. Soc. Rev.* **2011**, *40*, 5084 – 5121.

[45] a) G. Triola, G. Fabriàs, J. Casas, A. Llebaria, *J. Org. Chem.* **2003**, *68*, 9924 – 9932; b) S. De Jonghe, I. Lamote, K. Venkataraman, S. A. Boldin, U. Hillaert, J. Rozenski, C. Hendrix, R. Busson, D. De Keukeleire, S. Van Calenbergh, A. H. Futerman, P. Herdewijn, *J. Org. Chem.* **2002**, *67*, 988 – 996; c) I. Van Overmeire, S. A. Boldin, K. Venkataraman, R. Zisling, S. De Jonghe, S. Van Calenbergh, D. De Keukeleire, A. H. Futerman, P. Herdewijn, *J. Med. Chem.* **2000**, *43*, 4189 – 4199; d) L. He, H.-S. Byun, R. Bittman, *J. Org. Chem.* **2000**, *65*, 7627 – 7633.

[46] a) A. Singh, H.-J. Ha, J. Park, J. H. Kim, W. K. Lee, *Bioorg. Med. Chem.* **2011**, *19*, 6174 – 6181; b) H.-J. Ha, M. Ch. Hong, S. W. Ko, Y. W. Kim, W. K. Leeb, J. Park, *Bioorg. Med. Chem. Lett.* **2006**, *16*, 1880 – 1883.

[47] A. W. McDonagh, P. V. Murphy, *Tetrahedron* **2014**, *70*, 3191 – 3196.

[48] U. Hillaert, S. Boldin-Adamsky, J. Rozenski, R. Busson, A. H. Futerman, S. Van Calenbergh, *Bioorg. Med. Chem.* **2006**, *14*, 5273 – 5284 and references therein.

[49] M. Moreno, C. Murruzzu, A. Riera, *Bioorg. Med. Chem.* **2011**, *19*, 5184 – 5187 and references therein.

[50] a) Y. Salma, S. Ballereau, C. Maaliki, S. Ladeira, N. Andrieu-Abadie, Y. Génisson, *Org. Biomol. Chem.* **2010**, *8*, 3227 – 3243; b) Y. Salma, S. Ballereau, S. Ladeira, C. Lepetit, R. Chauvin, N. Andrieu-Abadie, Y. Génisson, *Tetrahedron* **2011**, *67*, 4253 – 4262.

[51] a) S. D. Karyakarte, T. P. Smith, S. R. Chemler, *J. Org. Chem.* **2012**, *77*, 7755 – 7760; b) R. Ramanujam, S. Ganjihal, N. Kalyanam, M. Majeed, *Tetrahedron: Asymmetry* **2013**, *24*, 663 – 668.

[52] For recent review in this field, see: J. Rentner, M. Kljajic, L. Offner, R. Breinbauer, *Tetrahedron* **2014**, *70*, 8983.

[53] For representative examples using this protocol see: a) S. Michelliza, A. Al-Mourabit, A. Gateau-Olesker, C. Marazano, *J. Org. Chem.* **2002**, *67*, 6474 – 6478; b) Y. L. Gol'Dfarb, B. P. Fabrichnyi, I. F. Shalavina, *Tetrahedron* **1961**, *17*, 21 – 36. For stereoselective reduction of 2,3-disubstituted and 2,3,4,5-tetrasubstituted thiophenes, see: c) P. A. Jacobi, M. Egberston, R. F. Frechette, S. Miao, C. K. K. T. Weiss, *Tetrahedron* **1988**, *44*, 3327 – 3338; d) P. A. Jacobi, R. F. Frechette, *Tetrahedron Lett.* **1987**, *28*, 2937 – 2940.

[54] P. Radha Krishna, B. Lavanya, A. Ilangovan, G. V. M. Sharma, *Tetrahedron: Asymmetry* **2000**, *11*, 4463 – 4472.

[55] a) P. Šafař, J. Žužiova, M. Bobošiková, Š. Marchalín, N. Pronayová, S. Comesse, A. Daïch, *Tetrahedron: Asymmetry* **2009**, *20*, 2137 – 2144; b) P. Šafař, J. Žužiova, Š. Marchalín, E. Tothova, N. Pronayová, L. Švorc, V. Vrabel, A. Daïch, *Tetrahedron: Asymmetry* **2009**, *20*, 626 – 634; c) Š. Marchalín, J. Žužiova, K. Kadlečikova, P. Šafař, P. Baran, V. Dalla, A. Daïch, *Tetrahedron Lett.* **2007**, *48*, 697 – 702.

[56] D. J. Baek, J.-H. Seo, C. Lim, J. H. Kim, D. H. Chung, W.-J. Cho, C.-Y. Kang, S. Kim, *ACS Med. Chem. Lett.* **2011**, *2*, 544 – 548.

[57] S. Combemale, C. Santos, F. Rodriguez, V. Garcia, C. Galaup, C. Frongia, V. Lobjois, T. Levade, C. Baudoin-Dehoux, S. Ballereau, Y. Genisson, *RSC Adv.* **2013**, *3*, 18970 – 18984.

Received: December 21, 2015
Published online on March 31, 2016

